



High catalytic activity of Co-Fe/α-Al₂O₃ in the steam reforming of toluene in the presence of hydrogen



Mitsuru Koike^a, Yuji Hisada^a, Lei Wang^a, Dalin Li^a, Hideo Watanabe^b, Yoshinao Nakagawa^a, Keiichi Tomishige^{a,*}

^a Department of Applied Chemistry, School of Engineering, Tohoku University, 6-6-07, Aoba, Aramaki, Aoba-ku, Sendai, 980-8579, Japan

^b Graduate School of Pure and Applied Sciences, University of Tsukuba, 1-1-1, Tennodai, Tsukuba, Ibaraki, 305-8573, Japan

ARTICLE INFO

Article history:

Received 5 February 2013

Received in revised form 29 March 2013

Accepted 29 April 2013

Available online 9 May 2013

Keywords:

Cobalt

Iron

Alloy

Steam reforming

Toluene

ABSTRACT

The addition of hydrogen to the reactant gas for the toluene steam reforming enhanced the stability and activity of Co-Fe/α-Al₂O₃ (Fe/Co = 0.25), which is due to the suppression of the oxidation of the bcc Co-Fe alloy phase as the catalytically active species. It is characteristic that the adsorption of hydrogen on Co-Fe/α-Al₂O₃ was much stronger than that on Co/α-Al₂O₃, suggesting that the coverage of adsorbed hydrogen species can be rather high under the reaction conditions. The kinetics analysis gave almost first reaction order with respect to toluene and higher reactivity of toluene than benzene indicate that the activated adsorption of toluene can proceed via its methyl group and it can be assisted by adsorbed hydrogen species at the bcc Co-Fe alloy surface.

© 2013 Elsevier B.V. All rights reserved.

1. Introduction

Utilization of biomass as renewable resources is very attractive from the viewpoint of the production of sustainable energies and chemicals [1–5]. Conversion of biomass to synthesis gas and hydrogen is one of essential technologies for the production of liquid fuels and chemicals with the environmental protection by the decrease of CO₂ emission [1–3,6–8]. In the utilization of syngas from biomass, tar impurity is the most serious problem because tar causes pollution of downstream equipments [3]. Tar is the mixture of various condensable organic compounds such as aromatic, oxygen-containing compounds and so on [3,9,10]. In non-catalytic gasification system, high reaction temperature is necessary for the reduction of the tar amount, and therefore air has been conventionally used as a gasifying agent, although the product gas is diluted with nitrogen [2]. Compared with the non-catalytic system, catalytic steam gasification at lower reaction temperature enables the production of highly-concentrated syngas without nitrogen dilution. In the system, biomass was pyrolyzed in non-catalytic process producing mainly tar, which is gasified with steam reforming over catalysts. Recently, various Co-based catalysts have been reported to show the high performance in the steam reforming of oxygenates

[11–16] hydrocarbons [17,18] and biomass-derived tar [19–22] as well as Ni-based catalysts [23–36]. In addition, the promoting effect of Fe addition to Ni catalysts in the steam reforming has been reported [37–40], and the additive effect of Fe to Co catalysts has been investigated [41–45]. We have also reported that Co-Fe/α-Al₂O₃ catalyst with optimum composition (Fe/Co = 0.25) showed higher catalytic activity and resistance to coke deposition than Co/α-Al₂O₃ in the steam reforming of tar derived from cedar wood [41]. In contrast, the performance of Co-Fe/α-Al₂O₃ catalyst was lower than that of Co/α-Al₂O₃ in the steam reforming toluene without hydrogen addition; toluene is a typical model compound of tar derived from biomass [3,9,46–48]. According to the catalyst characterization [41], both fcc and bcc Co-Fe alloys were formed by the reduction pretreatment in Co-Fe/α-Al₂O₃ catalyst. The bcc Co-Fe alloy phase disappeared after toluene steam reforming without hydrogen addition, on the other hand, in toluene steam reforming with hydrogen addition, Co-Fe/α-Al₂O₃ showed high catalytic performance and maintained the bcc Co-Fe alloy phase after the catalytic use. These results suggest that the bcc phase has a contribution to high catalytic performance. The steam reforming of hydrocarbons, in particular, aromatic compounds, under rather high partial pressure of hydrogen has been investigated mainly for two situations: one is the cracking or steam reforming of residual tar in the biomass gasification system at high temperature and the other is the steam reforming of the tar contained in the coke oven gas supplied from the coke production from coal used in the steel production process. The gasification of biomass at higher

* Corresponding author. Tel.: +81 227957214; fax: +81 227957214.

E-mail addresses: tomi@erec.che.tohoku.ac.jp, tomi@tulip.sannet.ne.jp (K. Tomishige).

temperature produces gas with relatively high partial pressure of hydrogen, meanwhile, tar by-product is also present in the product gas which mainly contains aromatic compounds [3]. One of technologies for the removal of the tar is catalytic steam reforming, and for this purpose, the catalytic performance has been evaluated under the reaction conditions in the presence of high partial pressure of hydrogen in the gas phase [49–51]. On the other hand, the coke oven gas has very high partial pressure of hydrogen ($\geq 50\%$) and the concentration of tar from the coke pyrolysis is relatively high [52,53]. For the purpose of the hydrogen production from the coke oven gas, the catalysts have been tested in the steam reforming of aromatics such as 1-methylnaphthalene under the presence of high partial pressure of hydrogen (for example, 80%) [54]. From the aspects mentioned above, the steam reforming of toluene in the presence of hydrogen can be important to widen the applicability of the catalysts. However, the role of the added hydrogen on the activity and the interaction between hydrogen and catalyst surface was not elucidated at all.

In this article, the effect of hydrogen addition to the reactant gas in the steam reforming of toluene was investigated in more details comparing between Co/ α -Al₂O₃ and Co-Fe/ α -Al₂O₃ (Fe/Co = 0.25). The interaction between hydrogen and Co-Fe/ α -Al₂O₃ was evaluated by the temperature programmed desorption of the adsorbed hydrogen, and stronger interaction was found than the case of Co/ α -Al₂O₃. Furthermore, the reaction mechanism is also discussed on the basis of the steam reforming reaction rate of toluene and benzene, and suggested that the adsorbed hydrogen can promote the chemisorption of toluene at the methyl group.

2. Experimental

2.1. Catalyst preparation

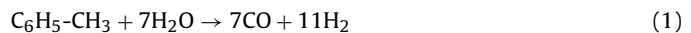
The procedures of the catalyst preparation were the same as those reported in the previous paper [41]. The support material of α -Al₂O₃ was prepared by the calcination of γ -Al₂O₃ (KHO-24, Sumitomo Chemical Co., Ltd., 133 m² g⁻¹, grain size 2–3 mm) in air at 1423 K. After the calcination, it was crushed and sieved to particle sizes between 0.3 and 0.6 mm. The Co-Fe/ α -Al₂O₃ catalyst was prepared by a co-impregnation method using a mixed aqueous solution of Co(NO₃)₂·6H₂O (Wako) and Fe(NO₃)₃·9H₂O (Wako). After the impregnation, the samples were dried at 383 K for 12 h followed by the calcination at 773 K for 3 h under air atmosphere. Loading amount of Co on the Co-Fe/ α -Al₂O₃ and Co/ α -Al₂O₃ catalysts was fixed at 12 wt% Co (as Co⁰ after complete reduction) and the loading amount of Fe was 0.25 as the molar ratio of Fe to Co (Fe/Co). Monometallic Co/ α -Al₂O₃ catalyst was also prepared with the same procedure using Co(NO₃)₂·6H₂O as the precursor. BET surface area of Co-Fe/ α -Al₂O₃ and Co/ α -Al₂O₃ was determined to be 12.8 and 9.8 m² g⁻¹, respectively.

2.2. Steam reforming of toluene and benzene without and with the addition of hydrogen to the reactant gas

Steam reforming of toluene and benzene was conducted in the continuous flow reaction system using a fixed catalyst bed reactor. The procedures and the analysis method were almost the same as reported previously [35]. Catalyst weight was 50 or 100 mg and the reaction was conducted after the reduction with H₂ at 773 K for 0.5 h in the reactor. In this study, we investigated the steam reforming of toluene and benzene without or with hydrogen addition to the reactant gas. The reaction temperature was 873 K. The molar ratio of steam to carbon was S/C = 1.7 and 3.4, and W/F = 0.05–1.1 g h/mol, where F represents the total flow rate of steam, N₂, H₂ and toluene (or benzene). The partial pressure of

hydrogen in effluent gas was determined by TCD-GC in the case without hydrogen addition. On the other hand, when the hydrogen was added to the reactant gas, it was difficult to determine partial pressure of produced hydrogen by TCD-GC. Therefore, when the amount of deposited carbon was negligible, the formation rate of produced hydrogen was calculated from the reaction schemes [55] as shown below. The details of the calculation procedures for the estimation of the formation rate of hydrogen are described in Supplementary information.

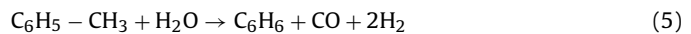
Steam reforming of toluene:



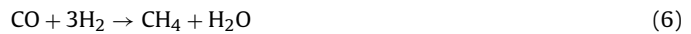
Steam reforming of benzene:



Steam dealkylation:



CO methanation:



Other reactions except for those listed above may be contributable, for example, steam dealkylation to CO₂ (C₆H₅-CH₃ + 2H₂O → C₆H₆ + CO₂ + 3H₂), hydrodealkylation (C₆H₅-CH₃ + H₂ → C₆H₆ + CH₄), hydrogenation, C-C hydrogenolysis and so on. The dealkylation reactions can be expressed by the combination of the steam dealkylation (Eq. (5)) and CO methanation (Eq. (6)), water gas shift (Eq. (2)–Eq. (1)) reactions and so on. Even at low toluene conversion under the present reaction conditions with and without hydrogen addition, the amount of the hydrogenation products such as methylcyclohexane, cyclohexane and that of their hydrogenolysis products such as alkanes were below the detection limit. This suggests that the steam reforming of toluene does not proceed via hydrogenation reactions. Therefore, these hydrogenation and hydrogenolysis reactions were not considered.

Regarding the catalysts used in the activity test for 80 min, the amount of the deposited coke was measured by the thermogravimetry (Thermo plus EVO II, Rigaku). After the test, a part of the catalyst (ca. 10 mg) was taken out from the catalyst bed. Thermogravimetric analysis (TGA) profiles were obtained in the air atmosphere at the heating rate of 10 K/min. Exothermic weight loss was observed at the temperature range between 600 and 900 K. This can be assigned to the combustion of deposited carbon [56–59]. It is possible to estimate the amount of deposited carbon on the basis of this weight loss.

2.3. Catalyst characterization

Temperature-programmed reduction (TPR) with H₂ was performed in the fixed-bed flow reactor. The TPR profile of each sample was recorded from room temperature to 1273 K under a flow of 5.0% H₂/Ar, and the flow rate was 30 ml/min. The sample weight was 50 mg. The pretreatment condition of samples was calcination at 773 K, reduction at 773 K or catalytic use. After the pretreatment, these samples were cooled down to room temperature under the nitrogen and then the sample was transferred to the TPR apparatus in the air atmosphere. The heating rate was 10 K/min and the temperature was maintained at 1273 K for 30 min after it reached 1273 K. The consumption of H₂ was monitored continuously with TCD equipped with frozen acetone trap in order to remove H₂O

from the effluent gas. The amount of H_2 consumption was estimated from the peak area in the TPR profiles.

Powder X-ray diffraction (XRD) patterns of the freshly reduced and used catalysts were collected using a Rigaku, Ultima IV using Cu K α ($\lambda = 0.154$ nm) generated at 40 kV and 20 mA. The amount of samples was about 50–100 mg. According to Vegard's law [60], the lattice constant of solid solution alloy is given from a linear combination of the lattice constant of each component. The lattice constants of fcc Co metal 0.3537 nm [61], fcc Fe metal 0.3646 nm [62], bcc Co metal 0.2827 nm [63] and bcc Fe 0.2867 nm [64] were used for the calculation. From the comparison between the line of Vegard's law and the d spacings obtained from the experimental results of XRD, it is possible to estimate the actual composition of each alloy phase.

Temperature-programmed desorption (TPD) of hydrogen on $Co-Fe/\alpha-Al_2O_3$ ($Fe/Co = 0.25$) and $Co/\alpha-Al_2O_3$ was analyzed using a fixed bed flow reaction system equipped with a quadrupole mass spectrometer (QMS, QMA200; Pfeiffer Vacuum Technology AG). 100 mg of catalysts was put in the quartz tube reactor (i.d. 4 mm). After the reduction under a flow of gas mixture of H_2/He (30/30 ml/min) at 773 K for 30 min, these samples were maintained at 773 K in a He (60 ml/min) gas flow for 30 min, and then these samples cooled down to room temperature. After the pulses of hydrogen were introduced to the catalyst by using a six-way valve, the samples were heated to 1173 K (heating rate: 10 K/min). The desorbed hydrogen was monitored continuously with QMS ($m/z = 2$).

2.4. Pulse reaction of H_2O decomposition and steam reforming of propane

Pulse reaction of steam reforming of propane over $Co-Fe/\alpha-Al_2O_3$ ($Fe/Co = 0.25$) and $Co/\alpha-Al_2O_3$ was conducted with the same

system described in H_2 -TPD. As a reference, the pulse reaction of steam with the catalysts was also tested. 30 mg of catalysts was put in the quartz tube reactor (i.d. 4 mm). After the reduction under a flow of gas mixture of H_2/He (30/30 ml/min) at 773 K for 30 min, the sample was heated to 873 K in a He (240 ml/min) gas flow. Then pulses of $H_2O +$ propane or H_2O were introduced to the catalyst with a six-way valve in the steam reforming of propane and the reaction of H_2O with the catalyst, respectively. H_2O was supplied by the gas stripping method. The composition of a pulse was 3.08 μmol $H_2O + 0.28 \mu\text{mol}$ $C_3H_8 + 25.4 \mu\text{mol}$ He or 3.08 μmol $H_2O + 25.7 \mu\text{mol}$ He.

3. Results and discussion

3.1. Activity test

3.1.1. Catalytic performance of $Co-Fe/\alpha-Al_2O_3$ and $Co/\alpha-Al_2O_3$ in the steam reforming of toluene in the absence of hydrogen

Fig. 1 shows the W/F dependence of the steam reforming of toluene without adding the hydrogen at $S/C = 3.4$ and 1.7 over $Co/\alpha-Al_2O_3$ and $Co-Fe/\alpha-Al_2O_3$ ($Fe/Co = 0.25$) catalysts under steady-state conditions. As mentioned below, the activity was decreased with time on stream, and after some reaction time, the activity was almost constant, and this can be regarded as the steady-state activity. Toluene conversion and the CO selectivity were increased with increasing W/F , and CO_2 selectivity and H_2/CO ratio were decreased with increasing W/F . When W/F was above the point where the toluene conversion reached almost 100%, the selectivity to CO and CO_2 , and H_2/CO ratio became constant, here, the reactions reached the equilibrium. From the comparison between $Co-Fe/\alpha-Al_2O_3$ and $Co/\alpha-Al_2O_3$ in the range of low W/F , $Co-Fe/\alpha-Al_2O_3$ showed much lower toluene conversion than $Co/\alpha-Al_2O_3$.

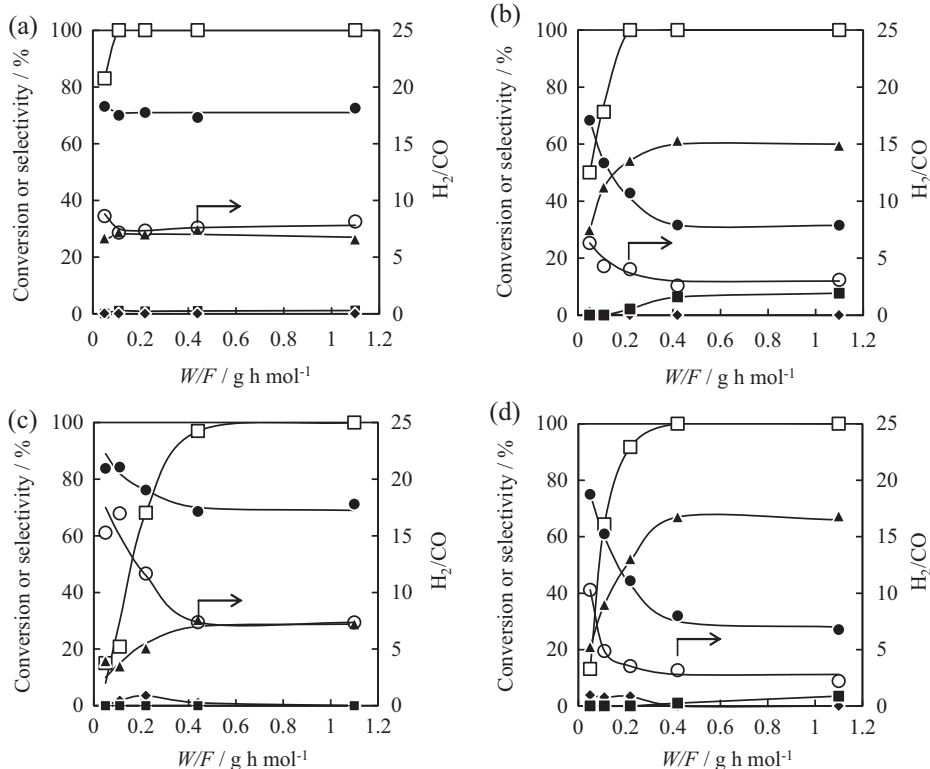


Fig. 1. Contact time (W/F) dependence of the conversion, selectivity and H_2/CO in steam reforming of toluene over (a and b) $Co/\alpha-Al_2O_3$ and (c and d) $Co-Fe/\alpha-Al_2O_3$ ($Fe/Co = 0.25$) catalysts under the steady-state conditions. (a and c) $S/C = 3.4$ (toluene/ $H_2O/N_2 = 1/23.6/56.9$ (molar ratio)), (b and d) $S/C = 1.7$ (toluene/ $H_2O/N_2 = 1/11.8/71.1$ (molar ratio)). □: toluene conversion, ▲: CO, ●: CO_2 , ■: CH_4 , ♦: benzene, ○: H_2/CO . Reaction conditions: $W = 100$ mg (50 mg catalyst was used under both of reaction condition ($S/C = 3.4$ and $W/F = 0.05$ g h/mol)), reaction temperature 873 K, reaction time 30 min, $W/F = 0.05$ –0.11 g/h/mol.

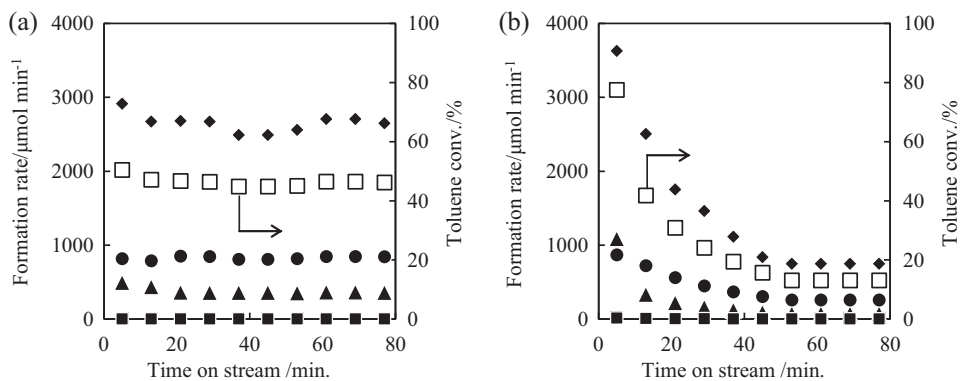


Fig. 2. Reaction time dependence of the formation rates of products and toluene conversion in steam reforming of toluene without hydrogen addition over (a) Co/α-Al₂O₃ and (b) Co-Fe/α-Al₂O₃ (Fe/Co = 0.25) catalysts at 873 K. □: toluene conversion, ▲: CO, ●: CO₂, ■: benzene, ◆: H₂. Reaction conditions: W = 100 mg, W/F = 0.05 g h/mol, S/C = 1.7 (toluene/H₂O/N₂ = 1/11.8/71.1 (molar ratio)).

On the other hand, the conversion difference between Co/α-Al₂O₃ and Co-Fe/α-Al₂O₃ became smaller at S/C = 1.7.

Fig. 2 shows the reaction time dependence of the formation rate of products and toluene conversion over Co-Fe/α-Al₂O₃ and Co/α-Al₂O₃ in steam reforming of toluene without hydrogen addition for 80 min (S/C = 1.7). On Co/α-Al₂O₃, the formation rate of the products was stable, and toluene conversion was kept at around 50% (Fig. 2a). In contrast, Co-Fe/α-Al₂O₃ catalyst showed about 80% toluene conversion at initial stage. The formation rate of products and toluene conversion at the initial stage were higher than those over Co/α-Al₂O₃. However, they decreased gradually with reaction time, and reached the steady state after 50 min. Under the steady-state conditions, the catalytic activity of Co-Fe/α-Al₂O₃ was lower than that of Co/α-Al₂O₃ as also shown in Fig. 1. There have been some reasons of the catalyst deactivation, and one reason is the coke deposition [6,65,66]. However, from TG analysis in air atmosphere, the amount of the deposited coke was determined to be less than 0.01 mmol g⁻¹-cat (<0.01% C-based yield) on the catalyst after the reaction in Fig. 2b. This result indicates that the Co-Fe/α-Al₂O₃ catalyst was not deactivated by the carbon deposition. Generally speaking, the coke formation tends to be more significant at lower S/C ratio. The Co-Fe/α-Al₂O₃ catalyst gave higher toluene conversion at lower S/C ratio (Fig. 1), and this also supports that the catalyst was deactivated by other reasons rather than by the coke deposition. In the steam reforming of hydrocarbons, higher partial pressure of steam as the reforming agent can give more oxidizing atmosphere. The lower activity of Co-Fe/α-Al₂O₃ than Co/α-Al₂O₃ under more oxidizing reaction conditions can be caused by the decrease of the reducibility of Co by the addition of Fe with higher

oxygen affinity [67]. Conversely, the performance of Co-Fe/α-Al₂O₃ under more reducing atmosphere was investigated.

3.1.2. Catalytic performance of Co-Fe/α-Al₂O₃ and Co/α-Al₂O₃ in the steam reforming of toluene in the presence of hydrogen

Fig. 3 shows the reaction time dependence of toluene steam reforming with hydrogen addition and lower S/C (1.7). The reaction conditions in Fig. 3 were the same as those in Fig. 2, except for the feeding rate of N₂ and H₂. The addition of H₂ compensated for the decrease of N₂, and the feeding rate of toluene and steam was unchanged. The addition of hydrogen to the reactant gas remarkably enhanced the steady-state activity of Co-Fe/α-Al₂O₃ in the toluene steam reforming from 13% (Fig. 2b) to 60% (Fig. 3b) as toluene conversion, and the promoting effect of hydrogen addition was also reported in previous report [68]. On the other hand, the addition of hydrogen decreased the activity of Co/α-Al₂O₃ from 45% (Fig. 2a) to 20% (Fig. 3a). The catalytic activity of Co-Fe/α-Al₂O₃ in toluene steam reforming with hydrogen addition was (Fig. 3b) even higher than that of Co/α-Al₂O₃ without hydrogen addition (Fig. 2a).

Next we investigated the effect of partial pressure of the hydrogen over Co-Fe/α-Al₂O₃. The conditions with higher steam partial pressure (S/C = 3.4) were applied, where the Co-Fe/α-Al₂O₃ catalyst shows lower activity. The results are shown in Fig. 4 and Table 1. The more stable and higher activity in toluene steam reforming of Co-Fe/α-Al₂O₃ was obtained under higher partial pressure of hydrogen added to the reactant gas. Comparing the results in Fig. 4 with the result in Fig. 3b indicates that higher partial pressure of hydrogen was needed to maintain the catalytic activity at higher S/C ratio.

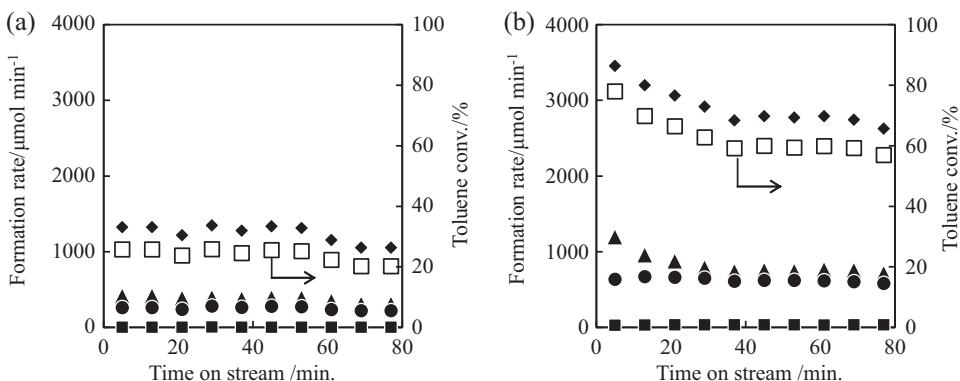


Fig. 3. Reaction time dependence of the formation rates of products and toluene conversion in steam reforming of toluene over (a) Co/α-Al₂O₃ and (b) Co-Fe/α-Al₂O₃ (Fe/Co = 0.25) catalysts at 873 K. □: toluene conversion, ▲: CO, ●: CO₂, ■: benzene, ◆: H₂. Reaction conditions: W = 100 mg, W/F = 0.05 g h/mol, S/C = 1.7 (toluene/H₂O/H₂ = 1/11.8/51.0/20.1 (molar ratio)).

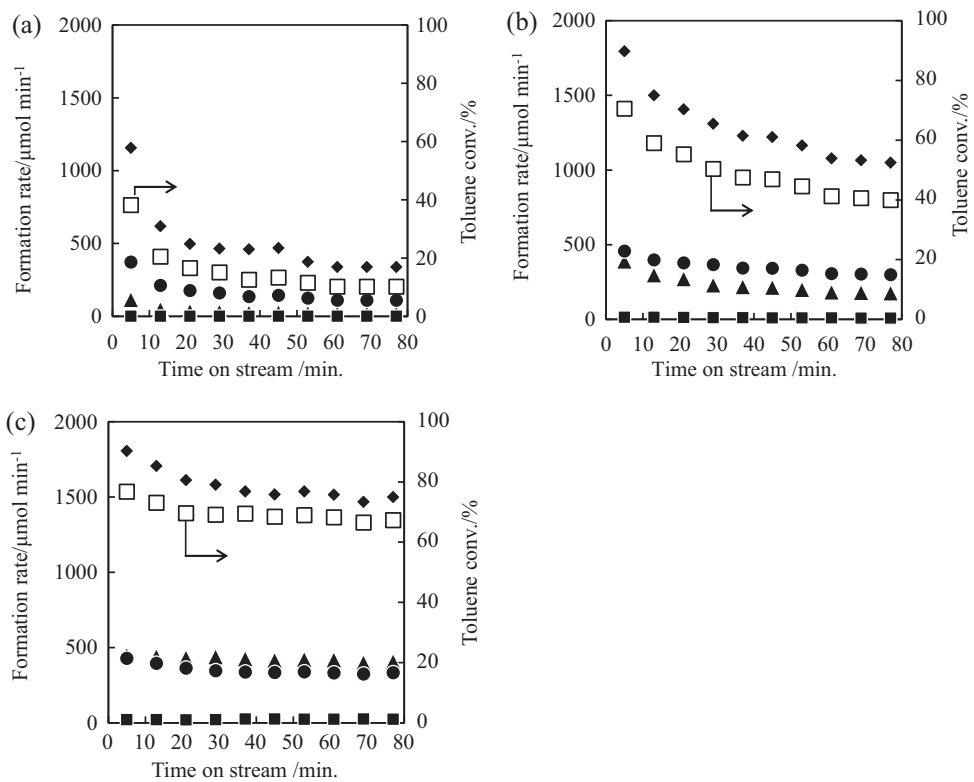


Fig. 4. Reaction time dependence of the formation rates of products and toluene conversion in steam reforming of toluene over Co-Fe/α-Al₂O₃ (Fe/Co=0.25) catalyst on various partial pressure of hydrogen. (toluene/H₂O/N₂/H₂ = (a) 1/23.6/56.9/0.0, (b) 1/23.6/37.0/19.9, (c) 1/23.6/0.0/56.9 (molar ratio)). □: toluene conversion, ▲: CO, ●: CO₂, ■: benzene, ♦: H₂. Reaction conditions: reaction temperature 873 K, W=50 mg, W/F=0.05 g h/mol, S/C=3.4.

Table 1
Steady-state catalytic performance in the steam reforming of toluene with and without hydrogen addition over Co-Fe/α-Al₂O₃.

Entry	Flow gas composition (mmol/min)				Toluene conv. (%)	Formation rate (μmol min⁻¹)				H ₂ /CO
	Toluene	H ₂ O	N ₂	H ₂		CO	CO ₂	Benzene	H ₂	
1	0.19	4.4	10.7	0.0	12.9	24	140	1	445	16.4
2	0.19	4.4	8.8	1.9	19.6	74	165	3	542	7.4
3	0.19	4.4	7.9	2.8	31.1	129	246	6	838	6.5
4	0.19	4.4	7.0	3.8	43.5	195	320	9	1134	5.8
5	0.19	4.4	5.1	5.6	52.0	255	340	15	1282	5.0
6	0.19	4.4	0.0	10.7	68.2	414	333	24	1512	3.6

Reaction conditions: reaction temperature 873 K, reaction time 80 min, W=50 mg, W/F=0.05 g h/mol, S/C=3.4 (toluene/H₂O/N₂+H₂=1/23.6/56.9 (molar ratio)).

3.2. Catalyst characterization

3.2.1. Characterization of catalysts after the reduction treatment and the catalytic use

Fig. 5A shows XRD patterns of Co-Fe/α-Al₂O₃ after reduction pretreatment and after the catalytic use in steam reforming of toluene for 5, 20 and 80 min. After the reduction pretreatment, both fcc and bcc Co-Fe alloys were detected (Fig. 5A, a). The assignment of these alloys is referred to our previous report [41]. The diffraction peak of the fcc Co-Fe alloy phase was not changed during reaction, however, the intensity of the diffraction peak of the bcc Co-Fe alloy phase decreased significantly with the reaction time and at the same time the peak position shifted to higher angle. Finally, the bcc Co-Fe alloy phase almost disappeared, suggesting that the bcc Co-Fe alloy was oxidized during the reaction. Fig. 5B shows the *d* spacing of fcc and bcc Co-Fe alloy phases as a function of the composition (Fe/(Co+Fe)) on Co-Fe/α-Al₂O₃ during activity test shown in Fig. 2b. The composition of the fcc and bcc Co-Fe alloy phases from Fig. 5 is summarized in Table 2. The obtained Fe/Co ratio in the fcc Co-Fe alloy phase increased slightly with reaction time of toluene steam reforming without hydrogen addition. The decrease

of the peak intensity of the fcc Co-Fe alloy phase was not so significant as that of the catalytic activity. Therefore, the change in the composition (Fe/Co) in the fcc alloy phase may not be related to the catalyst deactivation. In contrast, the decrease of the peak intensity of the bcc Co-Fe alloy phase was so significant as that of the catalytic activity. This suggests that bcc Co-Fe alloy phase contributes strongly to the catalytic activity, and the catalyst deactivation during the reaction is due to the decrease of the amount of the bcc alloy phase. Therefore, it is interpreted that the steady-state activity after 50 min can be originated from the fcc Co-Fe alloy phase. The composition of Fe/Co in the bcc Co-Fe alloy phase decreased with the reaction time and this can be interpreted by the preferential oxidation of the bcc Co-Fe alloy phase with higher Fe/Co, which is related to higher oxygen affinity of Fe than Co. One possible explanation of the increase in the Fe/Co ratio in the fcc Co-Fe alloy is the phase transition of the bcc Co-Fe with decreasing Fe/Co ratio to the fcc Co-Fe alloy phase. Totally, the oxidation of the metal phases can be connected to the catalyst deactivation [69–74].

In order to verify the oxidation of the alloy phase, H₂-TPR of Co-Fe/α-Al₂O₃ after toluene steam reforming was conducted, and profiles are shown in Fig. 6. Co-Fe/α-Al₂O₃ after the calcination

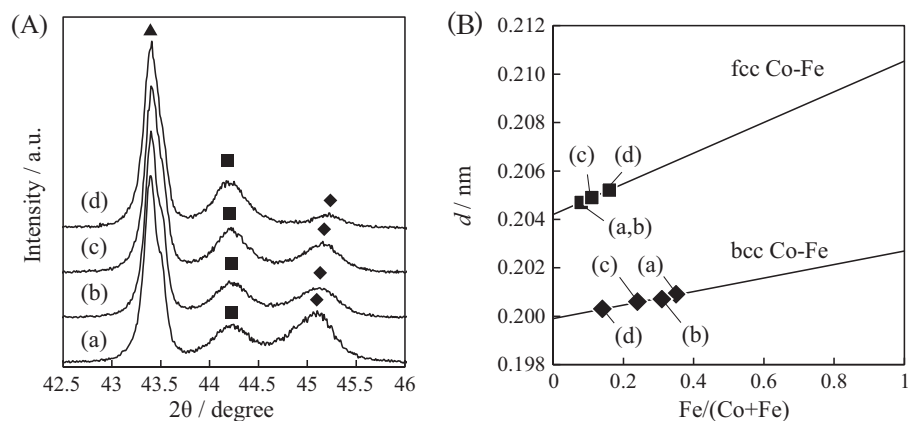


Fig. 5. (A) XRD patterns of Co-Fe/α-Al₂O₃ (Fe/Co = 0.25) after reduction and steam reforming of toluene, and (B) d spacing of the peaks of fcc Co-Fe and bcc C-Fe as a function of Fe/(Co + Fe). (a) After reduction pretreatment, after steam reforming of toluene for (b) 5 min, (c) 20 min and (d) 80 min during the activity test shown in Fig. 2b. ■: fcc Co-Fe solid solution alloy, ♦: bcc Co-Fe solid solution alloy, ▲: α-Al₂O₃. Reaction conditions: reaction temperature 873 K, W = 100 mg, W/F = 0.05 g h/mol, S/C = 1.7 (toluene/H₂O/N₂ = 1/11.8/71.1 (molar ratio)).

Table 2

Composition of fcc and bcc Co-Fe alloy phases on Co-Fe/α-Al₂O₃ (Fe/Co = 0.25) in toluene steam reforming without hydrogen addition (Fig. 2a).

Catalyst	Reaction time	Experimental ^a		Calculated Fe/(Co + Fe)		Calculated Fe/Co	
		$d_{\text{fccCo-Fe}}$ (nm)	$d_{\text{bccCo-Fe}}$ (nm)	fcc Co-Fe	bcc Co-Fe	fcc Co-Fe	bcc Co-Fe
Co-Fe/α-Al ₂ O ₃ (Fe/Co = 0.25)	0 min (after red.)	0.2047	0.2009	0.08	0.35	0.09	0.54
	5 min	0.2047	0.2007	0.08	0.31	0.09	0.45
	20 min	0.2049	0.2006	0.11	0.24	0.12	0.32
	80 min	0.2052	0.2003	0.16	0.14	0.18	0.16

^a Fig. 5.

and reduction were also shown in Fig. 6 as a reference. The results of H₂-TPR profiles are listed in Table 3. From the result in Fig. 2b, the amount of deposited carbon was determined to be less than 0.01 mmol g⁻¹-cat. Therefore, the hydrogen consumption by methanation of carbon species on Co-Fe/α-Al₂O₃ was estimated to be less than 0.02 mmol g⁻¹-cat and much smaller than that by reduction of metal oxide on Co-Fe/α-Al₂O₃. From these results, hydrogen consumption by methanation of carbon species can be negligible. The reduction of Co species on the calcined Co/α-Al₂O₃ finished below 773 K, in contrast, the reduction of Fe species on the calcined Fe/α-Al₂O₃ proceeded in a wide temperature range of 573–1173 K as reported previously [41]. In case of Co-Fe/α-Al₂O₃ after the calcination, the reduction of Fe was promoted by the coexistence of Co and the H₂ consumption peak was observed in the temperature range of 573–773 K (Fig. 6a). The amount of H₂ consumption was 3.2 mmol g⁻¹-cat, indicating that all the Co and Fe species were reduced on the basis of the assumption that Co and Fe are present as Co₃O₄ and Fe₃O₄, respectively, after calcination. Fig. 6b–e shows the TPR profiles of the catalysts after reduction and reaction, which were cooled down to room temperature after the treatment and then transferred to the TPR apparatus in the air atmosphere. The H₂ consumption peak was observed in the narrow temperature range of 500–700 K, which is assigned to the reduction

of the partially oxidized Co-Fe/α-Al₂O₃ during the sample transfer. The H₂ consumption was as small as 0.5 mmol g⁻¹-cat, suggesting that H₂ is consumed by the reduction of the surface oxide. On the other hand, another H₂ consumption peak was observed in the temperature range of 700–1000 K on the catalyst after the catalytic use. The H₂ consumption amount in the temperature range of 700–1000 K was increased with reaction time, which is considered as the reduction of the oxidized species during steam reforming reaction, and this oxidized species can be originated from the bcc Co-Fe alloy phase. Totally, after 80 min, it is estimated to be a third of Co + Fe amount (H₂ consumption 0.9 mmol g⁻¹-cat) oxidized during the reaction (Table 3).

3.2.2. Characterization after steam reforming of toluene with hydrogen addition

Fig. 7 shows the XRD patterns of Co-Fe/α-Al₂O₃ after the catalytic use in the steam reforming of toluene with hydrogen addition as listed in Table 4. Compared to the XRD pattern after toluene steam reforming without hydrogen addition at low S/C ratio (Fig. 5d), bcc Co-Fe alloy was completely oxidized at high S/C ratio (Fig. 7b). When the hydrogen was added to the reactant gas, the XRD peaks of bcc Co-Fe alloy phase was remained present with shift to smaller angle than that after reduction treatment, and the

Table 3

H₂ consumption of the catalysts in TPR.

Catalyst	Content (mmol g ⁻¹ -cat)		Pretreatment	H ₂ consumption in TPR (mmol g ⁻¹ -cat)		
	Co	Fe		L.T. (<700 K)	H.T. (700–1000 K)	Total ^a
Co-Fe/α-Al ₂ O ₃ (Fe/Co = 0.25)	2.0	0.5	Calcination	–	–	3.2
	2.0	0.5	Reduction	0.5	–	0.5
	2.0	0.5	Steam reforming for 5 min	0.4	0.2	0.6
	2.0	0.5	Steam reforming for 20 min	0.3	0.3	0.6
	2.0	0.5	Steam reforming for 80 min	0.4	0.5	0.9

^a H₂ consumption below 873 K in TPR profiles shown in Fig. 6.

Table 4

Composition of fcc and bcc Co-Fe alloy phases on Co-Fe/ α -Al₂O₃ (Fe/Co=0.25) and the distribution of Fe in each alloy after toluene steam reforming (Table 1).

Catalyst	Condition	Experimental ^a		Calculated Fe/(Co + Fe)		Calculated Fe/Co	
		$d_{\text{fccCo-Fe}}$ (nm)	$d_{\text{bccCo-Fe}}$ (nm)	fcc Co-Fe	bcc Co-Fe	fcc Co-Fe	bcc Co-Fe
Co-Fe/ α -Al ₂ O ₃ (Fe/Co=0.25)	Table 1, entry 1	0.2047	—	0.08	<0.01	0.09	<0.01
	Table 1, entry 2	0.2047	0.2006	0.08	0.24	0.09	0.32
	Table 1, entry 3	0.2047	0.2007	0.08	0.31	0.09	0.45
	Table 1, entry 4	0.2047	0.2008	0.08	0.33	0.09	0.49
	Table 1, entry 5	0.2047	0.2009	0.08	0.35	0.09	0.54
	Table 1, entry 6	0.2047	0.2009	0.08	0.35	0.09	0.54
	After reduction	0.2047	0.2009	0.08	0.35	0.09	0.54

^a Fig. 7.

shift decreased with increasing the partial pressure of hydrogen (Table 4). Higher partial pressure of the hydrogen suppressed the oxidation of the bcc Co-Fe alloy phase more remarkably. Considering that the XRD is not so sensitive to the surface state, the surface of the Co-Fe alloy phases may be oxidized to some extent. This is expectable from the slight deactivation observed in Fig. 4c.

Fig. 8 shows the results of the activity test in Co-Fe/ α -Al₂O₃ in the steam reforming of toluene without the hydrogen and subsequent test with the hydrogen. Here, the reaction conditions were just the same as those in Fig. 4. During the reaction without hydrogen, the activity decreased like that in Fig. 4a. On the other hand, when the hydrogen was added to the reactant gas just after the activity test in the toluene steam reforming without the hydrogen, the activity was almost the same as the steady-state activity in Fig. 4c where the test started just after reduction treatment. These results indicate that the oxidized species during the toluene steam reforming without hydrogen addition can be reduced with hydrogen and activated to give high activity. This behavior can be related to the TPR profile of the Co-Fe/ α -Al₂O₃ after reaction (Fig. 6e).

3.3. Pulse reaction of C₃H₈ + H₂O and H₂O

The activity of Co-Fe/ α -Al₂O₃ in the steam reforming of toluene was strongly influenced by the reaction conditions such as the presence of hydrogen, the ratio of steam to carbon, the reaction time and so on. The influence of the reaction conditions on the catalytic activity of Co/ α -Al₂O₃ can be different from that of Co-Fe/ α -Al₂O₃. Therefore, the catalytic behavior is apparently complex. In order to make the comparison easier, we tried to evaluate the catalytic

activity of the reduced catalysts using the pulse experiment technique. Table 5 lists the results of the pulse reaction of C₃H₈ + H₂O or H₂O on the reduced Co-Fe/ α -Al₂O₃ and Co/ α -Al₂O₃. Here, the amount of the reactants was smaller than that of metal and the surface metal (H₂ adsorption), and the results can be reflected by the

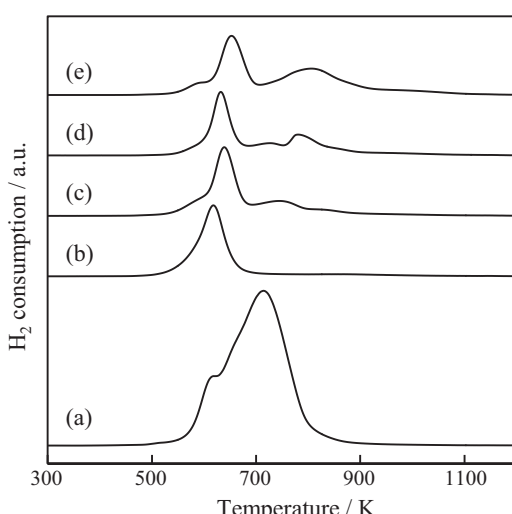
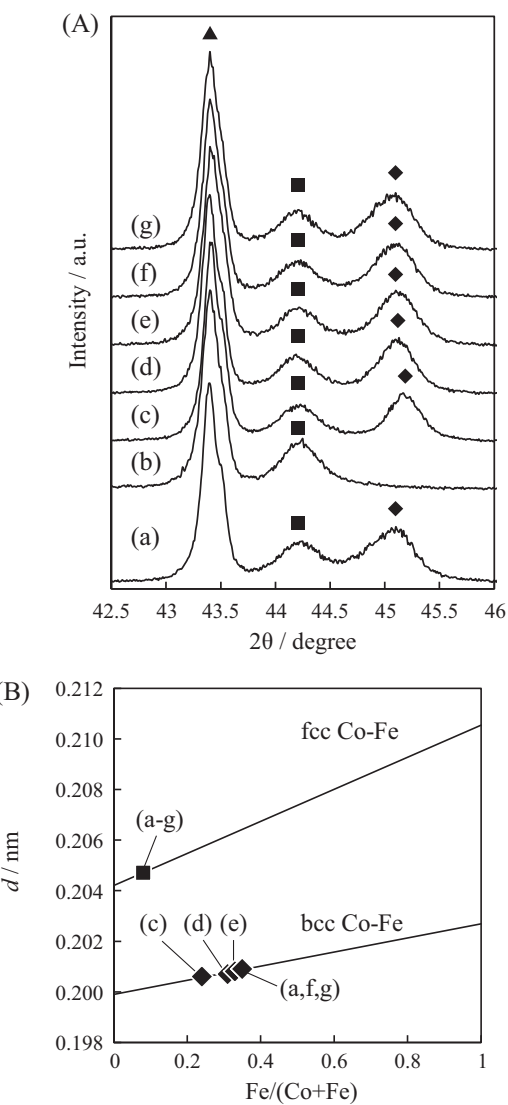


Fig. 6. TPR profiles of Co-Fe/ α -Al₂O₃ (Fe/Co = 0.25) catalysts in various conditions. (a) After the calcination pretreatment, (b) after the reduction pretreatment, after steam reforming of toluene for (c) 5 min, (d) 20 min and (e) 80 min. TPR conditions: heating rate 10 K/min, 5%H₂/Ar flow rate 30 ml/min. Sample weight: 50 mg.

Fig. 7. (A) XRD patterns of Co-Fe/ α -Al₂O₃ (Fe/Co=0.25) after steam reforming of toluene, and (B) d spacing of the peaks of fcc Co-Fe and bcc Co-Fe as a function of Fe/(Co + Fe). (a) After reduction pretreatment, (b) after steam reforming of toluene without hydrogen addition (Table 1, entry 1), (c–g) after steam reforming of toluene with hydrogen addition (Table 1, entries 2–6). ■: fcc Co-Fe solid solution alloy, ♦: bcc Co-Fe solid solution alloy, ▲: α -Al₂O₃.

Table 5

Pulse reactions of $C_3H_8 + H_2O$ and H_2O over $Co/\alpha-Al_2O_3$ and $Co-Fe/\alpha-Al_2O_3$ catalyst.

Catalysts	Content (μmol)		H_2 adsorption ^a (μmol)	Reactant (μmol)		Amount of reacted propane (μmol)	Yield (μmol)				
	Co	Fe		Propane	H_2O		CO	CH_4	CO_2	H_2	Calculated H_2 ^b
$Co/\alpha-Al_2O_3$	60	–	0.9	0.28	3.08	0.24	0.59	0.01	0.12	2.33	1.80
		–		–	3.08	–	–	–	–	0.50	–
$Co-Fe/\alpha-Al_2O_3$ ($Fe/Co = 0.25$)	60	15	1.4	0.28	3.08	0.20	0.54	0.02	0.05	3.44	1.43
		–		–	3.08	–	–	–	–	2.01	–

Reaction conditions: $W = 30$ mg, reaction temperature 873 K, carrier 240 ml/min He.

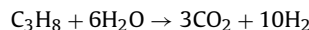
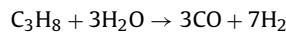
^a H_2 adsorption amount was estimated from H_2 -TPD (Fig. 10).

^b Calculated from CO, CH_4 , CO_2 and propane yield in propane steam reforming.

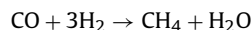
activity of the reduced catalysts, which corresponds to the initial activity in the experiments using the continuous flow reactor.

The steam reforming of propane gave CO, CH_4 , CO_2 and H_2 , and the formation routes are described below.

Propane steam reforming:



CO methanation:



Based on these reaction routes, the formation amount of H_2 can be calculated and the obtained values are also listed as “calculated H_2 ” in Table 5. The difference between the yield of H_2 and that of calculated H_2 can be interpreted by the catalyst oxidation with steam. In order to verify the contribution of the catalyst oxidation with steam, we also carried out the pulse H_2O reaction without the presence of C_3H_8 . The amount of H_2 yield in the H_2O reaction agreed well with the difference between the yield of H_2 and the calculated H_2 in the $C_3H_8 + H_2O$ reaction of both catalysts. The larger amount of H_2 formation in the pulse reaction of H_2O on $Co-Fe/\alpha-Al_2O_3$ than that on $Co/\alpha-Al_2O_3$ can be explained by high oxygen affinity of Fe [67]. The yield of CO, CO_2 , and the calculated H_2 which is due to the propane steam reforming on $Co/\alpha-Al_2O_3$ was a little larger than that on $Co-Fe/\alpha-Al_2O_3$, indicating that the activity of $Co-Fe/\alpha-Al_2O_3$ is comparable to that of $Co/\alpha-Al_2O_3$ in the reduced state. In addition, from the comparison between $Co/\alpha-Al_2O_3$ and $Co-Fe/\alpha-Al_2O_3$ in the H_2 yield by the reaction with H_2O , the addition of Fe enhanced the reactivity of H_2O , and Fe-rich bcc Co-Fe alloy can exhibit the high reactivity of H_2O . This property can be connected to the oxidation of Fe-rich bcc Co-Fe alloy during the

steam reforming without hydrogen addition. The oxidation of Fe species in the bcc Co-Fe alloy with steam leads to oxidized Fe and H_2 , and the oxidized Fe species can be reduced to metallic Fe species with hydrogen, in particular, in the steam reforming with hydrogen addition. This means that the oxidation of Fe^0 with steam and the reduction of Fe^{n+} with hydrogen are in an equilibrium state. As shown in Fig. 4, rather high hydrogen pressure is necessary for the shift of the equilibrium to the reduced side and this can be due to the high oxygen affinity of Fe [67].

As listed in Table 1, the catalytic activity of toluene steam reforming in $Co-Fe/\alpha-Al_2O_3$ was higher under higher partial pressure of the hydrogen, and the toluene conversion was 68.2% at toluene/ $H_2O/N_2/H_2 = 1/23.6/0/57.0$ and $W/F = 0.05$ g h/mol. On the other hand, $Co/\alpha-Al_2O_3$ gave 83% toluene conversion in the toluene steam reforming without hydrogen addition at similar reaction conditions shown in Fig. 1a. The toluene conversion on $Co-Fe/\alpha-Al_2O_3$ with hydrogen addition is comparable to that on $Co/\alpha-Al_2O_3$, and this behavior agreed with the behavior in the pulse reaction of the $C_3H_8 + H_2O$. This suggests that the toluene steam reforming reaction in the presence of larger amount of hydrogen proceeds on $Co-Fe/\alpha-Al_2O_3$ in more reduced state.

As a result, high activity can be obtained in the case of the maintenance of the bcc Co-Fe alloy. This means that the shift to the reduced Fe side in the equilibrium of the oxidation of Fe^0 with steam and the reduction of oxidized Fe with a reductant. In the toluene steam reforming with hydrogen addition, added hydrogen plays a role as the reductant. On the other hand, in the steam reforming of tar without hydrogen addition, $Co-Fe/\alpha-Al_2O_3$ showed higher activity than $Co/\alpha-Al_2O_3$, and the bcc Co-Fe alloy was partially maintained and this can be connected to the reforming activity. The maintenance of bcc Co-Fe alloy in the reduced state can be explained by tar itself as a reductant because tar can contain the compounds with high reducing ability such as aldehydes, ketones and carboxylic acids [3].

3.4. Reaction kinetics and mechanism of toluene steam reforming in the presence of hydrogen over $Co-Fe/\alpha-Al_2O_3$ ($Fe/Co = 0.25$) catalyst

In order to discuss the reaction mechanism of the toluene steam reforming in the presence of hydrogen over $Co-Fe/\alpha-Al_2O_3$, we measured the kinetics in toluene steam reforming with hydrogen addition. Fig. 9 shows the results of the kinetics measurement regarding toluene and steam. Here, $Co-Fe/\alpha-Al_2O_3$ catalyst was diluted with inert $\alpha-Al_2O_3$ (5 mg catalyst + 45 mg $\alpha-Al_2O_3$) and used. Under these experimental conditions, the toluene conversion became low ($\leq 30\%$) enough to measure the reaction rate. The reaction order with respect to toluene and steam was estimated to be 0.8 and -0.5 , respectively, as shown by the lines in Fig. 9. The almost first reaction order with respect to toluene suggests that the coverage of toluene is low and the activated adsorption of toluene can be a rate-determining step, and this behavior agreed well with

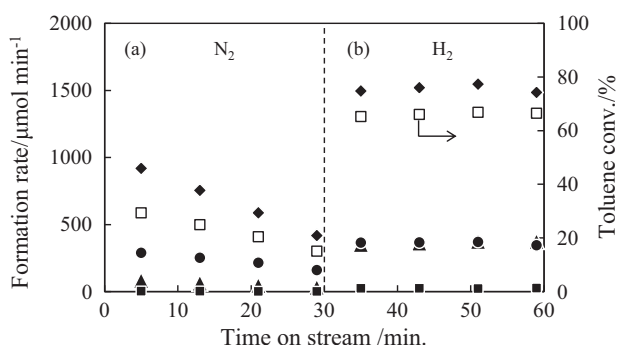


Fig. 8. Reaction condition dependence of the formation rates of products and toluene conversion in steam reforming of toluene over $Co-Fe/\alpha-Al_2O_3$ ($Fe/Co = 0.25$) catalyst at 873 K. □: toluene conversion, ▲: CO, ●: CO_2 , ■: benzene, ◆: H_2 . Reaction conditions: $W = 50$ mg, $W/F = 0.05$ g h/mol, $S/C = 3.4$ (toluene/ $H_2O/N_2/H_2$ = (a) $1/23.6/56.9/0.0$, (b) $1/23.6/0.0/56.9$ (molar ratio)).

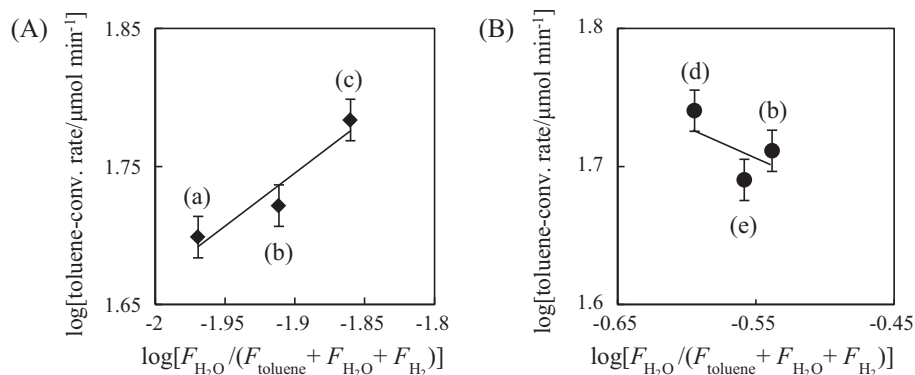


Fig. 9. Toluene steam reforming rate versus partial pressure of (a) toluene and (b) H_2O in the toluene steam reforming with the addition of hydrogen on Co-Fe/α-Al₂O₃ (Fe/Co = 0.25). Reaction conditions: $W = 50 \text{ mg}$ (5 mg catalyst + 45 mg α-Al₂O₃), $W/F = 0.05 \text{ g h/mol}$, reaction temperature 873 K, feeding rate: (a) toluene 0.16 mmol/min, steam 4.4 mmol/min, H_2 10.8 mmol/min, (b) toluene 0.19 mmol/min, steam 4.4 mmol/min, H_2 10.7 mmol/min, (c) toluene 0.21 mmol/min, steam 4.4 mmol/min, H_2 10.7 mmol/min, (d) toluene 0.19 mmol/min, steam 3.9 mmol/min, H_2 11.2 mmol/min, (e) toluene 0.19 mmol/min, steam 4.2 mmol/min, H_2 10.9 mmol/min.

the results reported previously [75–77]. When the toluene activation such as dissociative adsorption ($\text{C}_6\text{H}_5\text{CH}_3 \rightarrow \text{C}_6\text{H}_5\text{CH}_2 + \text{H}$) is a rate-determining step, the reaction order with respect to H_2 can be strongly negative, as respected in the case of methane reforming over Ni catalysts [78]. In fact, Co/α-Al₂O₃ gave negative reaction order with respect to hydrogen as shown in Figs. 2a and 3a.

It is characteristic that the reaction order with respect to H_2O over Co-Fe/α-Al₂O₃ was determined to be negative. On the other hand, it has been reported that the reaction order with respect to steam was close to zero in the toluene steam reforming over Ni/olivine [75] and commercial nickel-based catalyst [76,77]. Negative reaction order with respect to steam on Co-Fe/α-Al₂O₃ can be caused by the oxidation of the surface Fe atoms on the Co-Fe alloy particles, which can decrease the rate of the toluene activation. When the partial pressure of hydrogen was increased, it is thought that the adsorbed oxygen species on the Fe atoms can be removed by H_2 . Therefore, hydrogen can promote the toluene steam reforming by maintaining Fe in the reduced state. However, if the reaction order with respect to hydrogen can be negative on the reduced surface of Co-Fe/α-Al₂O₃, high activity in the toluene steam reforming with hydrogen addition should not be obtained as also mentioned above. These results suggest that the interaction between H_2 and catalyst surface is different on Co-Fe/α-Al₂O₃ and Co/α-Al₂O₃, therefore, the H₂-TPD was measured.

The profiles of H₂-TPD are shown in Fig. 10. The desorption of adsorbed hydrogen on Co/α-Al₂O₃ was observed in the range of 450–670 K. In contrast, that on Co-Fe/α-Al₂O₃ was observed in the wider range of 450–950 K. The amounts of the desorbed hydrogen on Co/α-Al₂O₃ and Co-Fe/α-Al₂O₃ were 14 and 27 $\mu\text{mol g}^{-1}\text{cat}$, respectively, which is supported by our previous report [41]. The desorbed hydrogen species at higher temperature than 670 K on Co-Fe/α-Al₂O₃ (Fe/Co = 0.25) can be due to the Fe addition. In the previous report [79], high desorption temperature of H_2 from Fe/SiO₂ has been observed in the temperature range of 573–973 K in the H₂-TPD. Based on the results and previous report [79], the hydrogen desorption at lower and higher temperature can be caused by the phase of fcc Co-Fe with higher Co content and bcc Co-Fe with higher Fe content, respectively. This result indicates that the adsorption of hydrogen on Co-Fe/α-Al₂O₃ is very strong and this behavior suggests that the coverage of the adsorbed hydrogen species on Co-Fe/α-Al₂O₃ is very high even under the reaction conditions, in particular, in the presence of the hydrogen. This property can be connected to high steam reforming activity of toluene of Co-Fe/α-Al₂O₃ even in the presence of hydrogen.

3.5. Comparison between steam reforming of toluene and benzene

The kinetic analysis of toluene steam reforming indicates that the activation of toluene is an important step. It is known that the energy of benzyl C–H bond is rather low, therefore, it is thought that the weak C–H bond can contribute to the activated adsorption of toluene. In order to evaluate the effect of this weak C–H bond, we compared the performance in the steam reforming of toluene and benzene (Table 6). In case of Co/α-Al₂O₃, the steam reforming without hydrogen addition was tested (Table 6, entries 1 and 2). The reaction rate of toluene was slightly higher than that of benzene. The slight difference in the reactivity of toluene and benzene suggests that the activation of C–H bond on the aromatic ring can be a rate-determining step. The adsorbed hydrogen species on Co metal surface can suppress the dissociative adsorption of benzene and toluene, which is supported by the result that hydrogen addition to the toluene steam reforming decreased the activity of Co/α-Al₂O₃ significantly (Figs. 2a and 3a). On the other hand, in the case of Co-Fe/α-Al₂O₃ (Fe/Co = 0.25) catalyst, with the hydrogen addition (Table 6, entries 3 and 4), the reactivity of toluene was much higher than that of benzene. These results indicate that the contribution of methyl group in toluene to the activated adsorption on Co-Fe/α-Al₂O₃ is clearly larger than that on Co/α-Al₂O₃. Under the reaction conditions of the steam reforming of benzene and toluene with hydrogen addition, the amount of the hydrogenation product

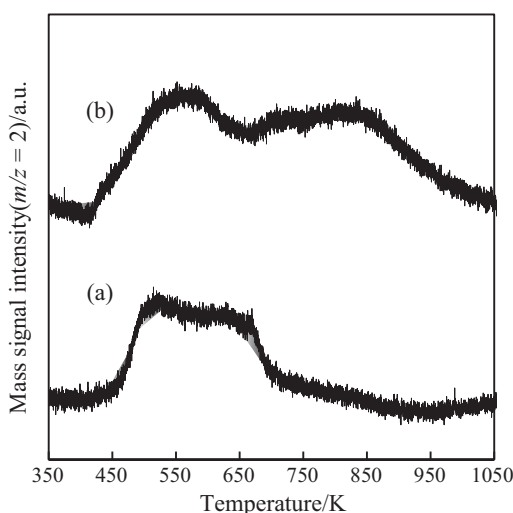


Fig. 10. TPD profiles of H_2 on (a) Co/α-Al₂O₃ and (b) Co-Fe/α-Al₂O₃ (Fe/Co = 0.25) catalyst TPD conditions: heating rate 10 K/min, He flow rate 60 ml/min. Sample weight 100 mg.

Table 6

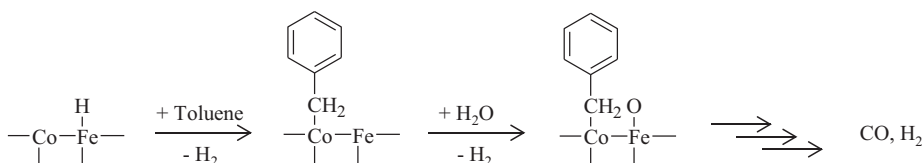
Steady-state catalytic performance in the steam reforming of benzene and toluene over Co/α-Al₂O₃ and Co-Fe/α-Al₂O₃.

Entry	Catalysts	Flow gas composition (mmol/min)					Benzene or toluene conv. (%)	Formation rate (μmol min ⁻¹)				H ₂ /CO
		Benzene	Toluene	H ₂ O	N ₂	H ₂		CO	CO ₂	Benzene	H ₂	
1	Co/α-Al ₂ O ₃	0.45	–	4.4	26.8	0.0	40.9	242	859	–	2385	9.8
2	–	–	0.38	4.4	26.8	0.0	46.2	359	843	2	2648	7.4
3	Co-Fe/α-Al ₂ O ₃ (Fe/Co = 0.25)	0.45	–	4.4	19.2	7.6	25.5	314	373	–	1402	4.5
4	–	–	0.38	4.4	19.2	7.6	56.9	715	582	34	2626	3.7

Reaction conditions: reaction temperature 873 K, reaction time 80 min, W = 100 mg, W/F = 0.05 g h/mol, S/C = 1.7 (benzene/H₂O/N₂ + H₂ = 1/9.9/59.7, toluene/H₂O/N₂ + H₂ = 1/11.8/71.1 (molar ratio)).

such as cyclohexane and methylcyclohexane was below the detection limit. The steam reforming of benzene and toluene may consist of the hydrogenation of the substrates to cyclohexane and methylcyclohexane and the consecutive steam reforming of the cyclohexanes. Judging from no detection of the cyclohexanes during the reactions, the hydrogenation of the substrates should be the rate-determining step. However, difference in the reactivity of benzene and toluene in the hydrogenation reaction cannot be so large, and this cannot explain the results in Table 6 entries 3 and 4. Therefore, it is thought that toluene and benzene are activated directly, not via hydrogenation reaction. This discussion suggests the toluene activation via methyl group.

An important point is that high activity of toluene steam reforming of Co-Fe/α-Al₂O₃ (Fe/Co = 0.25) in the presence of hydrogen can be caused by the synergy over bcc Co-Fe alloy surface. The presence of hydrogen can suppress the oxidation of Fe species on the Co-Fe alloy phase with steam. The metallic surface of the bcc Co-Fe alloy has a strong interaction with hydrogen and the coverage of adsorbed hydrogen species can be maintained to be high. At present, we think that this hydrogen species can help the activation of toluene via its methyl group. The proposed reaction step is described below.



The adsorbed hydrogen species may enhance the activated adsorption of toluene, although the further investigation is necessary to verify this reaction scheme.

4. Conclusions

1. The activity of Co-Fe/α-Al₂O₃ (Fe/Co = 0.25) decreased with time on stream in the steam reforming of toluene without the addition of hydrogen. It was verified that the deactivation is caused by the oxidation of the bcc Co-Fe alloy phase.
2. The addition of hydrogen to the reactant gases in toluene steam reforming on Co-Fe/α-Al₂O₃ (Fe/Co = 0.25) suppressed the deactivation remarkably and Co-Fe/α-Al₂O₃ exhibited high activity in toluene steam reforming in the presence of hydrogen. On the other hand, Co/α-Al₂O₃ showed much lower activity in the presence of hydrogen than in the absence.
3. The toluene steam reforming in the presence of hydrogen over Co-Fe/α-Al₂O₃ gave first and negative reaction order with respect to toluene and steam, respectively, suggesting that the activation of toluene is an important elementary step.

4. The adsorption of hydrogen on the bcc Co-Fe alloy surface on Co-Fe/α-Al₂O₃ is so strong that the coverage of adsorbed hydrogen species may be rather high in the toluene steam reforming with the addition of hydrogen.
5. The adsorption of toluene can proceed at the methyl group and it can be assisted by adsorbed hydrogen species at the bcc Co-Fe alloy surface.

Acknowledgement

This work was in part supported by the Cabinet Office, Government of Japan through its “Funding Program for Next Generation World-Leading Researchers”.

Appendix A. Supplementary data

Supplementary data associated with this article can be found, in the online version, at <http://dx.doi.org/10.1016/j.apcatb.2013.04.065>.

References

- [1] G.W. Huber, S. Iborra, A. Corma, Chemical Reviews 106 (2006) 4044.
- [2] A.V. Bridgwater, Applied Catalysis A: General 116 (1994) 5.
- [3] H. de Las, E. Salaises, J. Mazumder, R. Lucky, Chemical Reviews 111 (2011) 5404.
- [4] A. Corma, S. Iborra, A. Velty, Chemical Reviews 107 (2007) 2411.
- [5] R.R. Davda, J.W. Shabaker, G.W. Huber, R.D. Cortright, J.A. Dumesic, Applied Catalysis B: Environmental 56 (2005) 171.
- [6] D. Dayton, A Review of the Literature on Catalytic Biomass Tar Destruction, December, NREL/TP-510-32815, 2002, Available on Internet.
- [7] D. Li, Y. Nakagawa, K. Tomishige, Chinese Journal of Catalysis 33 (2012) 583.
- [8] K. Tomishige, M. Asadullah, K. Kunimori, Catalysis Today 89 (2004) 389.
- [9] D. Świerczyński, S. Libs, C. Courson, A. Kiennemann, Applied Catalysis B: Environmental 74 (2007) 211.
- [10] K. Polychronopoulou, K. Giannakopoulos, A.M. Efstratiou, Applied Catalysis B: Environmental 111 (2012) 360.
- [11] K. Urasaki, K. Tokunaga, Y. Sekine, M. Matsukata, E. Kikuchi, Catalysis Communications 9 (2008) 600.
- [12] N. Iwasa, S. Masuda, N. Takezawa, Reaction Kinetics and Catalysis Letters 55 (1995) 349.
- [13] C.K. Cheng, S.Y. Foo, A.A. Adesina, Catalysis Communication 12 (2010) 292.
- [14] B. Zhang, X. Tang, Y. Li, Y. Xu, W. Shen, International Journal of Hydrogen Energy 32 (2007) 2367.
- [15] X. Hu, G. Lu, Journal of Molecular Catalysis A: Chemical 261 (2007) 43.
- [16] L. He, H. Berntsen, E. Ochoa-Fernandez, J. Walmsley, E. Blekkan, D. Chen, Topics in Catalysis 52 (2009) 206.
- [17] T. Furusawa, A. Tsutsumi, Applied Catalysis A: General 278 (2005) 207.

- [18] T. Furusawa, A. Tsutsumi, *Applied Catalysis A: General* 278 (2005) 195.
- [19] K. Tasaka, T. Furusawa, A. Tsutsumi, *Energy and Fuels* 21 (2007) 590.
- [20] K. Tasaka, T. Furusawa, A. Tsutsumi, *Chemical Engineering Science* 62 (2007) 5558.
- [21] L. Wang, D. Li, M. Koike, H. Watanabe, Y. Xu, Y. Nakagawa, K. Tomishige, *Fuel* (2013), <http://dx.doi.org/10.1016/j.fuel.2012.01.073>, in press.
- [22] D. Li, C. Ishikawa, M. Koike, L. Wang, Y. Nakagawa, K. Tomishige, *International Journal of hydrogen energy* 38 (2013) 3572.
- [23] N. Iwasa, T. Yamane, M. Takei, J. Ozaki, M. Arai, *International Journal of Hydrogen Energy* 35 (2010) 110.
- [24] Y. Sekine, D. Mukai, Y. Murai, S. Tochiya, Y. Izutsu, K. Sekiguchi, N. Hosomura, H. Arai, E. Kikuchi, Y. Sugiura, *Applied Catalysis A: General* 451 (2013) 160.
- [25] D. Mukai, S. Tochiya, Y. Murai, M. Imori, T. Hashimoto, Y. Sugiura, Y. Sekine, *Applied Catalysis A: General* 453 (2013) 60.
- [26] T. Furusawa, Y. Miura, Y. Kori, M. Sato, N. Suzuki, *Catalysis Communication* 10 (2009) 552.
- [27] T. Furusawa, K. Saito, Y. Kori, Y. Miura, M. Sato, *Fuel* 103 (2013) 111.
- [28] D. Li, Y. Nakagawa, K. Tomishige, *Applied Catalysis A: General* 408 (2011) 1.
- [29] T. Kimura, T. Miyazawa, J. Nishikawa, T. Miyao, S. Naito, K. Okumura, K. Kunimori, K. Tomishige, *Applied Catalysis B: Environmental* 68 (2006) 160.
- [30] T. Miyazawa, T. Kimura, J. Nishikawa, S. Kado, K. Kunimori, K. Tomishige, *Catalysis Today* 115 (2006) 254.
- [31] K. Tomishige, T. Kimura, T. Miyazawa, J. Nishikawa, K. Kunimori, *Catalysis Communication* 8 (2007) 1074.
- [32] J. Nishikawa, T. Miyazawa, K. Nakamura, M. Asadullah, K. Kunimori, K. Tomishige, *Catalysis Communication* 9 (2008) 195.
- [33] J. Nishikawa, K. Nakamura, M. Asadullah, T. Miyazawa, K. Kunimori, K. Tomishige, *Catalysis Today* 131 (2008) 146.
- [34] K. Nakamura, T. Miyazawa, T. Sakurai, T. Miyao, S. Naito, N. Begum, K. Kunimori, K. Tomishige, *Applied Catalysis B: Environmental* 86 (2009) 36.
- [35] M. Koike, C. Ishikawa, D. Li, L. Wang, Y. Nakagawa, K. Tomishige, *Fuel* 103 (2013) 122.
- [36] D. Li, L. Wang, M. Koike, Y. Nakagawa, K. Tomishige, *Applied Catalysis B: Environmental* 102 (2011) 528.
- [37] L. Wang, M. Koike, S. Koso, Y. Nakagawa, K. Tomishige, *Applied Catalysis A: General* 392 (2011) 248.
- [38] M. Koike, D. Li, Y. Nakagawa, K. Tomishige, *ChemSusChem* 5 (2012) 2312.
- [39] D. Świerczyński, C. Courson, L. Bedel, A. Kiennemann, J. Guille, *Chemistry of Materials* 18 (2006) 4025.
- [40] R.P. Fiua, M.A. Silva, J.S. Boaventura, *International Journal of Hydrogen Energy* 35 (2010) 11216.
- [41] L. Wang, Y. Hisada, M. Koike, D. Li, H. Watanabe, Y. Nakagawa, K. Tomishige, *Applied Catalysis B: Environmental* 86 (2012) 95.
- [42] A. Kazama, Y. Sekine, K. Oyama, M. Matsukata, E. Kikuchi, *Applied Catalysis A: General* 383 (2010) 96.
- [43] Y. Sekine, A. Kazama, Y. Izutsu, M. Matsukata, E. Kikuchi, *Catalysis Letters* 132 (2009) 329.
- [44] J.A. Torres, J. Llorca, A. Casanovas, M. Domínguez, J. Salvadó, D. Montané, *Journal of Power Sources* 169 (2007) 158.
- [45] M.M. Natile, F. Poletto, A. Galenda, A. Glisenti, T. Montini, L. Rogatis, P. Fornasiero, *Chemistry of Materials* 20 (2008) 2314.
- [46] J. Srinakruang, K. Sato, T. Vitidsant, K. Fujimoto, *Catalysis Communication* 6 (2005) 437.
- [47] T.A. Milne, R.J. Evans, N. Abatzoglou, Biomass Gasifier "Tars": Their Nature, Formation, and Conversion, November, NREL/TP-570-25357, 1998, Available on Internet.
- [48] A. Łamacz, A. Krztoń, G. Djéga-Mariadassou, *Catalysis Today* 176 (2011) 347.
- [49] M. Virginie, C. Courson, D. Niznansky, N. Chaoui, A. Kienneman, *Applied Catalysis B: Environmental* 101 (2010) 90.
- [50] J.N. Kuhn, Z. Zhao, L.G. Felix, R.B. Slimane, C.W. Choi, U.S. Ozkan, *Applied Catalysis B: Environmental* 81 (2008) 14.
- [51] J. Hepola, P. Simell, *Applied Catalysis B: Environmental* 14 (1997) 287.
- [52] M. Onozaki, K. Watanabe, T. Hashimoto, H. Saegusa, Y. Katayama, *Fuel* 85 (2006) 143.
- [53] K. Miura, M. Kawase, H. Nakagawa, R. Ashida, T. Nakai, T. Ishikawa, *Journal of Chemical Engineering of Japan* 36 (2003) 735.
- [54] J. Yang, X. Wang, L. Li, K. Shen, X. Lu, W. Ding, *Applied Catalysis B: Environmental* 96 (2010) 232.
- [55] D. Duprez, *Applied Catalysis A: General* 82 (1992) 111.
- [56] K. Tomishige, Y. Himeno, Y. Matsuo, Y. Yoshinaga, K. Fujimoto, *Industrial & Engineering Chemistry Research* 39 (2000) 1891.
- [57] K. Tomishige, *Catalysis Today* 89 (2004) 405.
- [58] M. Nurunnabi, Y. Mukainakano, S. Kado, T. Miyao, S. Naito, K. Okumura, K. Kunimori, K. Tomishige, *Applied Catalysis A: General* 325 (2007) 154.
- [59] M. Nurunnabi, Y. Mukainakano, S. Kado, B. Li, K. Kunimori, K. Suzuki, K. Fujimoto, K. Tomishige, *Applied Catalysis A: General* 299 (2006) 145.
- [60] A.R. Denton, N.W. Ashcroft, *Physical Review A* 43 (1991) 3161.
- [61] X-Ray Powder Diffraction Data File ICDD 01-077-7456.
- [62] L.H. Bennett, B.C. Giessem, T.B. Massalski, *Alloy Phase Diagrams*, Material Research Society, Pittsburgh, PA, 1984.
- [63] G.A. Prinz, *Physical Review Letters* 54 (1985) 1051.
- [64] X-Ray Powder Diffraction Data File, ICDD 01-071-4409.
- [65] M. Nurunnabi, Y. Mukainakano, S. Kado, T. Miyazawa, K. Okumura, T. Miyao, S. Naito, K. Fujimoto, K. Suzuki, K. Kunimori, K. Tomishige, *Applied Catalysis A: General* 308 (2006) 1.
- [66] K. Tomishige, *Journal of the Japan Petroleum Institute* 50 (2007) 287.
- [67] T.B. Reed, *Free Energy Formation of Binary Compounds*, MIT Press, Cambridge, MA, 1971, pp. 66.
- [68] M. Virginie, C. Courson, A. Kiennemann, *Comptes Rendus Chimie* 13 (2010) 1319.
- [69] Y. Chen, K. Tomishige, K. Yokoyama, K. Fujimoto, *Applied Catalysis A: General* 165 (1997) 335.
- [70] Y. Chen, O. Yamazaki, K. Tomishige, K. Fujimoto, *Catalysis Letters* 39 (1996) 91.
- [71] Y. Matsuo, Y. Yoshinaga, Y. Sekine, K. Tomishige, K. Fujimoto, *Catalysis Today* 63 (2000) 439.
- [72] M. Nurunnabi, B. Li, K. Kunimori, K. Suzuki, K. Fujimoto, K. Tomishige, *Applied Catalysis A: General* 292 (2005) 272.
- [73] M. Nurunnabi, B. Li, K. Kunimori, K. Suzuki, K. Fujimoto, K. Tomishige, *Catalysis Letters* 103 (2005) 277.
- [74] Y. Mukainakano, K. Yoshida, S. Kado, K. Okumura, K. Kunimori, K. Tomishige, *Chemical Engineering Science* 63 (2008) 4891.
- [75] D. Swierczynski, C. Courson, A. Kiennemann, *Chemical Engineering and Processing* 47 (2008) 508.
- [76] J. Corella, J.M. Toledo, M. Aznar, *Industrial & Engineering Chemistry Research* 41 (2002) 3351.
- [77] A. Jess, *Chemical Engineering and Processing: Process Intensification* 35 (1996) 487.
- [78] N. Laosiripojana, S. Assabumrungrat, *Applied Catalysis A: General* 290 (2005) 200.
- [79] T. Ishihara, K. Eguchi, H. Arai, *Applied Catalysis* 40 (1988) 87.